Supplementary Information for "Coupled Folding and Binding of the Disordered Protein PUMA does not Require Particular Residual Structure".

Joseph M. Rogers, Chi T. Wong, Jane Clarke*

Department of Chemistry, University of Cambridge, Lensfield Road, Cambridge, CB2 1EW, U.K.

Methods

Protein expression and purification

Protein expression and purification of Mcl-1 was carried out as described elsewhere[1]. PUMA peptide, residues 127-161 (Uniprot Q99ML1) with the mutation M144A was used as the wild-type peptide in this study, similar to M144I pseudo wild-type used in the NMR structure[2] and the 34 amino acid peptide used in the previous kinetic characterization[1]. Unlike the M144I peptide, M144A was monomeric at all concentrations studied (Supplementary Fig. S3). Wild-type and mutant peptide were expressed as GB1 fusion proteins[1]. Protein expression was carried out in an identical manner to MCL-1[1], however, after binding to Ni^{2+}-agarose resin, the resin was additionally washed with 50 mM Tris pH 7.4, 100 mM NaCl, then 50 mM Tris pH 7.4, 100 mM NaCl, 5mM $CaCl_2$. Factor Xa (New England Biolabs) was added to release the peptide from the resin. The supernatant was then buffer exchanged, using desalting HiTrap (GE Healthcare), into 10 mM Tris pH 7.0 and bound to HiTrap Q. A linear gradient of NaCl was applied and peptide eluted at 7-10% 1 M NaCl. PUMA was further purified using gel filtration Superdex G30 (GE Healthcare) equilibrated in the experimental phosphate buffer. Peptides were filtered before $N_{2(l)}$, freezing and storage at -80 ˚C. Peptide concentration was determined using an extinction coefficient determined by amino acid analysis.

Buffers

All experiments were carried out in 50 mM sodium phosphate pH 7.0.

Circular dichroism

CD spectra were taken using Chirascan (Applied Photophysics), using a 2 mm path length cuvette. Estimates for the percentage helicity (%helix) were calculated using the average mean residue ellipticity at 222 nm, obtained using three concentrations of peptide, and Eq. 1[3].

$$\%Helix = 100 / (1 + ((Ellipticity - Ellipticity_{helix}) / (Ellipticity_{coil} - Ellipticity))) \quad [1]$$

A value of -725 deg cm^2 dmol $^{-1}$ was used for 100% random coil ($Ellipticity_{coil}$) and a value of –34100 deg cm^2 dmol $^{-1}$ was used for 100% helix in a 35 amino acid peptide ($Ellipticity_{helix}$)[3].

Association kinetics

Association was monitored using an SX18 or SX20 fluorescence stopped-flow spectrometer (Applied Photophysics) at 25˚C. Excitation at 280 nm and emission recorded above 305 nm. Proteins were mixed with PUMA in excess (minimum x10 fold) to set up pseudo-first-order conditions [4]. PUMA was used in excess as, with fewer fluorescent tryptophans, greater signal to noise ratio was achieved. A minimum of six kinetics traces were averaged and then fit to a single exponential function, Eq. 2,

$$F = F_{\infty} + \Delta F \exp(-k_{obs} t) \qquad [2]$$

where F is fluorescence at time t, F_{∞} the final fluorescence, ΔF is the fluorescence amplitude of the reaction, k_{obs} is the apparent rate constant. k_{obs} can be interpreted using Eq. 3.

$$k_{obs} = k_{-} + k_{+}[A]_0 \qquad [3]$$

where k- is the dissociation rate constant, k+ the association rate constant and $[A]_0$ the concentration of the protein in excess.

Dissociation kinetics

Dissociation kinetics were followed by pre-forming the PUMA peptide MCL-1 complex at 2.5-5 μM and manual mixing with a solution containing an excess (30-1000 fold) concentration of the peptide PUMA W133F N149A (M144A) which does not show any fluorescence change upon binding MCL-1. Fluorescence was followed using Cary Eclipse Fluorimeter (Aligent Technologies) at 25 ˚C. Data were fit to Eq. 2 with k_{obs}=k-. With sufficient excess of PUMA W133F N149A (M144A) the fit k_{obs} became essentially independent of the concentration of this peptide. Only k- in this regime were included in the average k-.

Fitting, Figures and Errors

All fitting was performed using ProFit (Quantum Soft). Figures were prepared using ProFit and Pymol. A 7% standard deviation on the PUMA peptide concentration was determined

using repeated amino acid analysis, this error was propagated through to the error in *k*+. Errors were propagated using standard equations.

Proline isomerization

Longer (50-100s) stopped-flow traces were taken to detect proline isomerization. All pseudo-first-order association traces were fit to a double exponential function, Eq. 4

$$F = F_{\infty} + \Delta F \exp\left(-k_{obs} t\right) + \Delta F_{pro} \exp\left(-k_{pro} t\right) \qquad [4]$$

which is identical to Eq. 2 with the addition of ΔF_{pro} the fluorescence amplitude due to proline isomerization and k_{pro} the concentration-dependent phase attributed to rate limiting proline isomerization.

Supplementary Results

Structural changes upon binding

As mentioned in the main text, CD spectra (Fig. S2) show that proline containing PUMA peptides are still able to occupy the helix conformations upon binding MCL-1. CD spectra are low-resolution and, upon proline mutation, small distortions, or fraying, of the helix may occur and remain undetected. However, a similar intrinsic fluorescence change upon binding is seen for all wild-type and proline containing mutants. It should be noted that a single mutation of PUMA, N149A, is sufficient to abolish the fluorescence change caused by the interaction of the peptide with MCL-1. This was taken advantage of in producing a suitable peptide (PUMA W133F+N149A) for out-competition studies. As asparagine is not detectably fluorescent when excited at 280 nm, it is likely that the presence of N149 leads to the observed fluorescence change by interacting with the cluster of tryptophan residues in MCL-1 (as can be seen in the structure pdb 2ROC). We would argue that this highly specific interaction, and the associated fluorescence change, would only occur if helical conformations (at C-terminal end of bound PUMA) were present for all bound, proline-containing, PUMA peptides. Some helical fraying, small enough to not be detected by low-resolution CD, at the N-terminus of bound, proline-containing PUMA cannot be ruled out.

Apparent two-state behaviour

Only one phase is observed during association experiments using stopped-flow and manual mixing/stopped-flow dissociation experiments, when binding is monitored using intrinsic fluorescence. This does not exclude the possibility of intermediate states being populated, either with interconversion rates too fast/slow for the above techniques, or with no spectroscopic change upon formation. The low K_d of wild-type PUMA binding MCL-1 is unsuitable for equilibrium titration studies, by isothermal titration calorimetry (ITC) or intrinsic fluorescence, due to the low concentrations required obtain data suitable for fitting. Proline containing mutants are also unsuitable for careful comparison between equilibrium and kinetic measurements due to the added complication of the (described below) cis-isomer state.
To confirm that two states in the kinetic experiments are the only states significantly populated, a structurally conservative mutant of PUMA (with single mutation L148A) was made and its binding to MCL-1 quantified. This mutant binds weaker than the wild-type, with a K_d range appropriate for both ITC and kinetic characterization. The K_d calculated from the

kinetic data (0.102 ± 0.008 μM) was very similar to that fit from ITC (two repeats 0.12 μM, 0.13 μM) (Fig. S4).

.

Proline isomerization

As stated in the main text, proline is unique amongst the natural amino acids due to its N-alkylation. However proline is unique for an additional reason, the significant population (10-40%) of the cis peptide bond conformation in unstructured states[5]. In the bound state of wild-type PUMA all peptide bonds are trans. However, when a proline mutation is made, similar to protein folding, isomerization of cis conformations might be expected to be rate limiting during association[5]. For association of proline mutants, with pseudo-first-order conditions and MCL-1 in excess, additional, slow, concentration-independent, kinetic phases are observed (Fig. S5). Only in two central positions, A139G and R143P, is this phase >5% total amplitude. Interestingly, this phase is not observable when PUMA is in excess, suggesting that any cis-peptide, upon collision with MCL-1, does not form a long-lasting complex that can impede the trans-peptide binding.

The association rate constants ($k+$) were obtained using pseudo-first-order conditions with mutant PUMA in excess, as described in *Methods*. If isomerization is present, then the concentration of binding competent peptide could be 5% lower than the (known) total concentration. As knowledge of PUMA concentration is required to calculate $k+$, the values of $k+$ proline mutant could be up to 5% higher than quoted in Table S1. This is comparable to the error in the PUMA concentration and does not affect the conclusions made in the main text.

Supplementary Figures

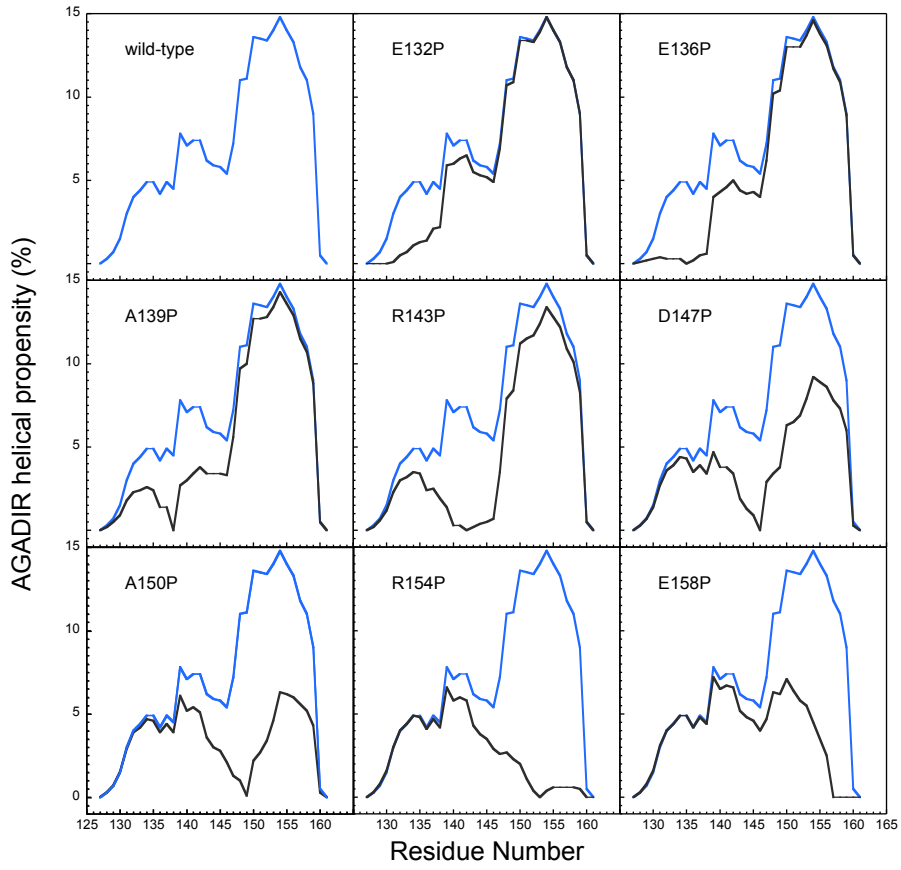

Fig. S1. AGADIR helical predictions. Wild-type shown in blue, mutant in black. All proline mutations reduce helicity to zero immediately N-terminal to the position of the substitution. Note that AGADIR predicts that the loss of overall helicity due to proline mutation would be greater towards the N-terminus however, as shown in Fig. 1C, the loss of helicity is relatively uniform across the peptide.

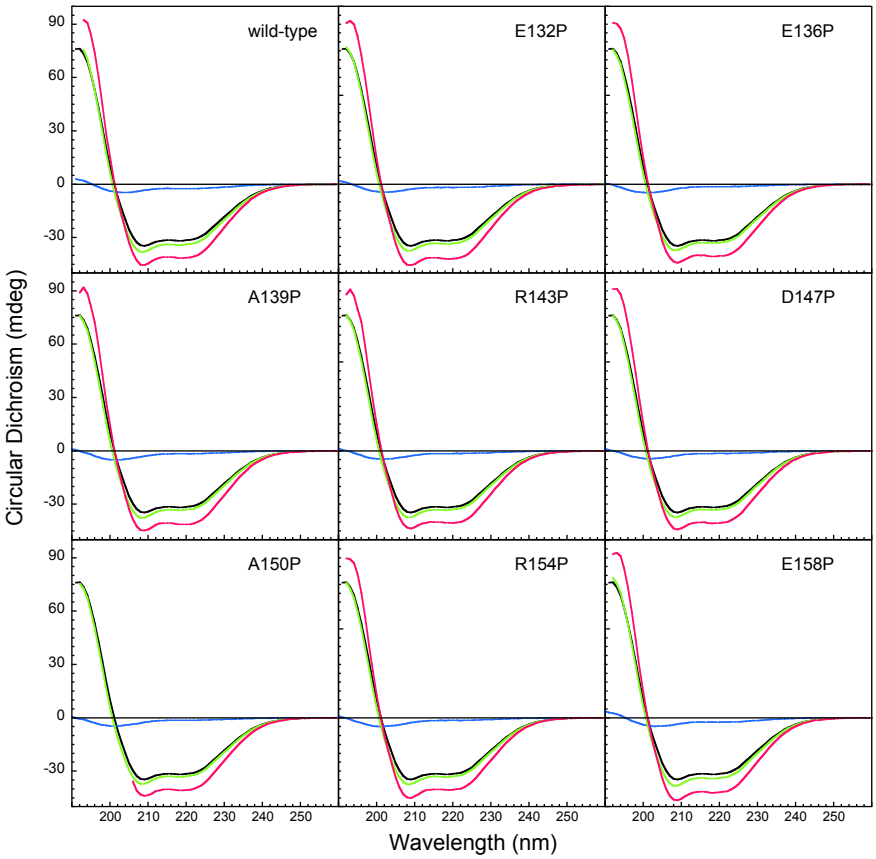

Fig. S2. All PUMA proline mutants bound to form a helical complex with MCL-1, similar to that made by wild-type PUMA. Circular dichroism spectra of wild-type or mutant PUMA (blue), MCL-1 (black) and their 1:1 molar ratio complex (magenta). The sum of the isolated PUMA and MCL-1 spectra, that expected if there were no interaction, is shown in green. All components are at 5 μM, apart from A150P complex which, due to that mutant's weaker binding, was recorded at 20 μM (then divided by 4 for comparison).

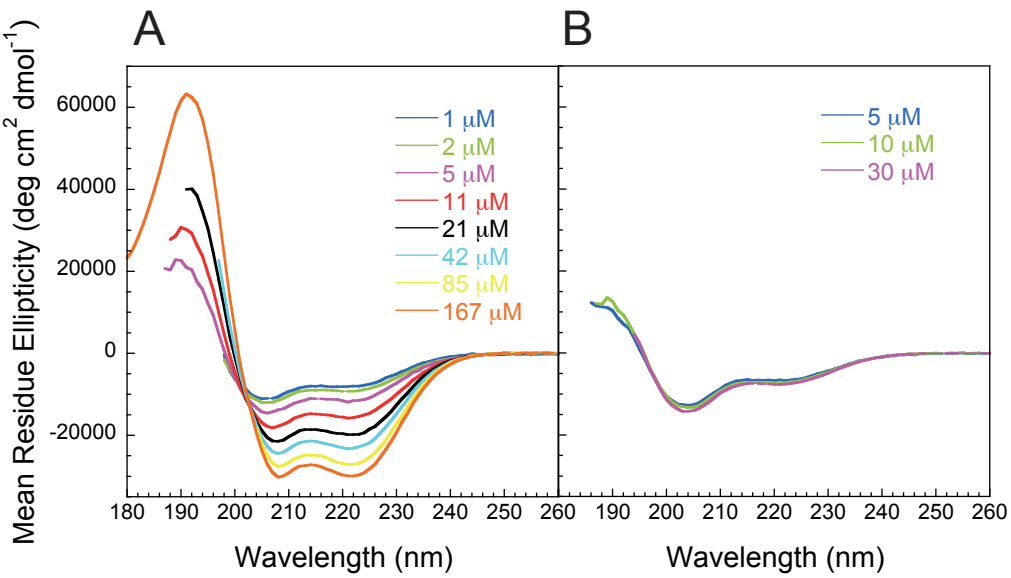

Fig. S3. The wild-type peptide used in this study does not undergo oligomerization. (A) Circular dichroism spectra of PUMA peptide 34 amino acids in length used in the previous kinetic study[1], with methionine at position 144, shows a strong dependence on concentration suggesting a helical oligomer. (B) Circular dichroism spectra of wild-type peptide used in this study, PUMA peptide 35 amino acids in length with alanine are position 144, does not show such oligomerization.

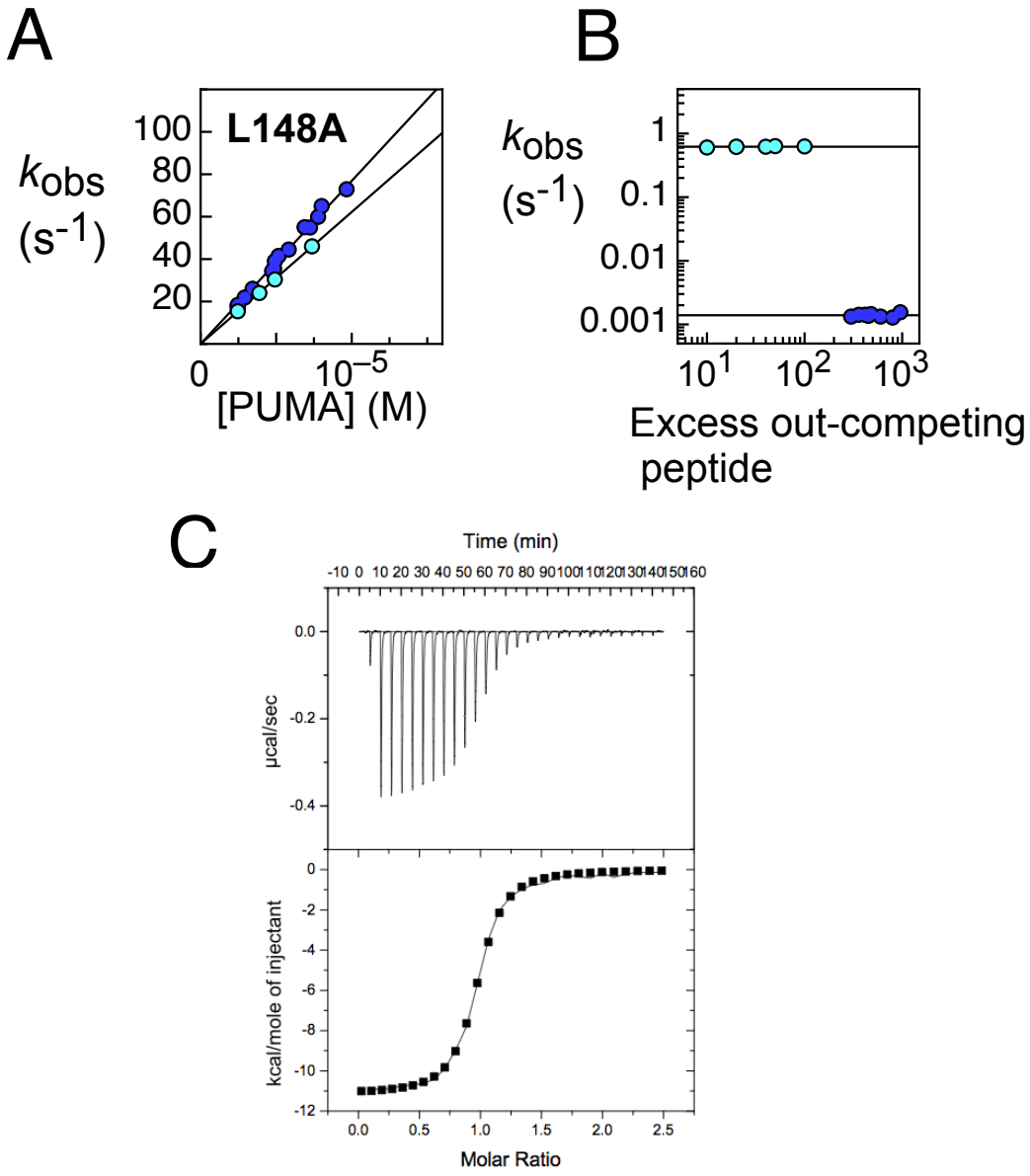

Fig. S4. Rate constants determined by fluorescence stopped-flow and ITC for PUMA L148A binding MCL-1. (A) Observed rate constants for the binding of PUMA wild-type (blue) and PUMA L148A (cyan) and wild-type MCL-1 . (B) Observed rate constants for the dissociation of PUMA L148A from MCL-1, triggered by a large excess of out-competing peptide. (C) ITC trace for PUMA L148A binding MCL-1, collected using VP-ITC (GE), PUMA peptide was in the syringe, MCL-1 was in the cell. Data analyzed using supplied Origin software (Originlab) and single site binding equation.

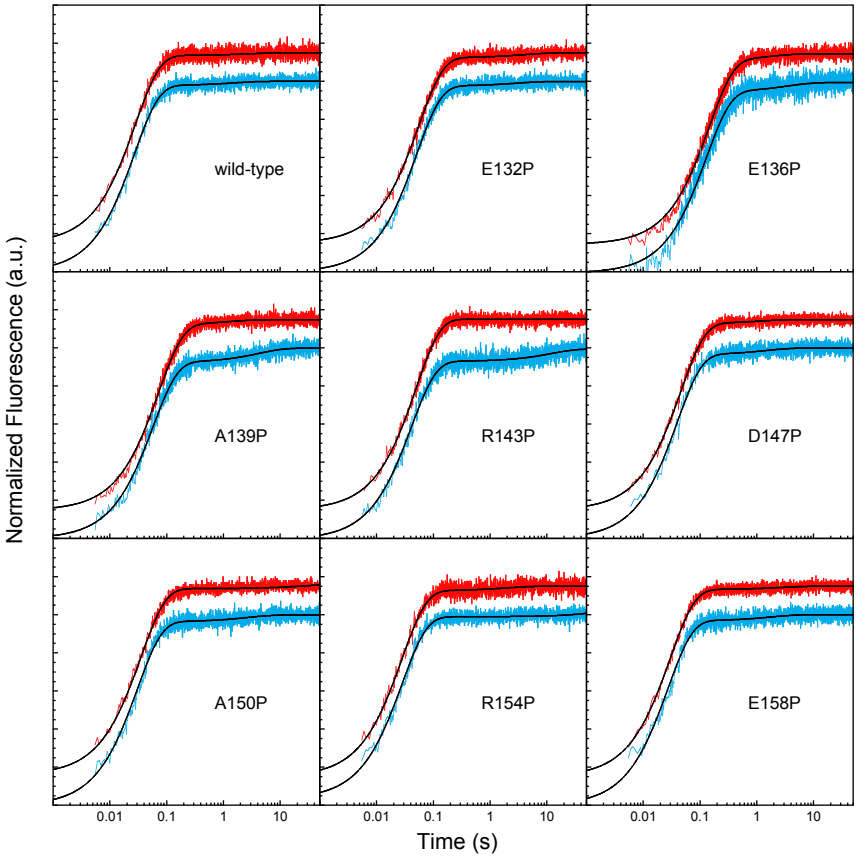

Fig. S5. Stopped-flow traces that show proline isomerization. Association between MCL-1 5 μM and PUMA mutant 0.5 μM (blue). Association of MCL-1 0.5 μM and PUMA mutant 5 μM (red). The first, larger amplitude, faster kinetic phase is due to the association of all trans peptide with MCL-1. The second, smaller amplitude, slower phase, clearly visible for A139P and R143P when MCL-1 is in excess (blue), and is attributed to cis peptide having to isomerize before association.

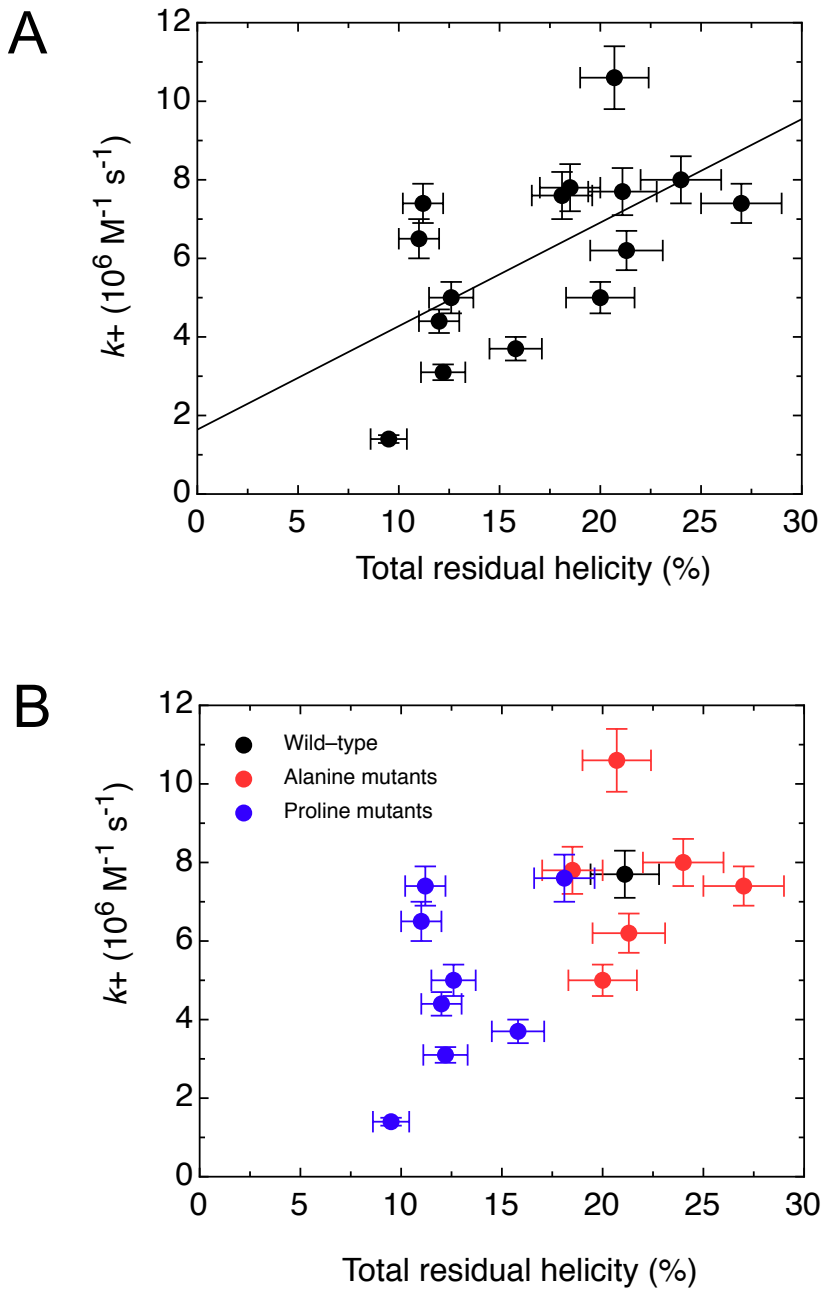

Fig. S6. Dependence of association rate constant (*k*+) on overall helicity. (A) A weak correlation (gradient 0.61 ± 0.07, Pearson's r = 0.6) can be observed between the association rate constant (*k*+) and the overall helicity of the PUMA peptide measured by CD. (B) Points separated into wild-type (black), alanine mutants (red) and proline mutants (purple).

Table S1.

Rate constants and equilibrium binding constants for wild-type and PUMA binding MCL-1. Experimental (measured by CD) and AGADIR predictions for the total/global residual helical content for unbound PUMA and PUMA mutants.

	$k+$ ($\times 10^6$ M^{-1} s^{-1})	$k-$ ($\times 10^{-3}$ s^{-1})	K_d (nM)	Experimental Residual Helicity (%)	AGADIR helical prediction (%)
Wild-type	7.7 (± 0.6)	1.39 (± 0.09)	0.18 (± 0.02)	21.1 (± 1.7)	7.5
E132A	5 (± 0.4)	1.34 (± 0.06)	0.27 (± 0.02)	20 (± 1.7)	7.4
E136A	6.2 (± 0.5)	3.1 (± 0.2)	0.5 (± 0.05)	21.3 (± 1.8)	8.9
R143A	10.6 (± 0.8)	1.59 (± 0.04)	0.149 (± 0.011)	20.7 (± 1.7)	7.0
D147A	7.4 (± 0.5)	1.31 (± 0.15)	0.18 (± 0.02)	27 (± 2)	7.8
R154A	7.8 (± 0.6)	2.2 (± 0.2)	0.28 (± 0.03)	18.5 (± 1.5)	4.8
E158A	8 (± 0.6)	1.09 (± 0.11)	0.136 (± 0.017)	24 (± 2)	7.3
E132P	3.7 (± 0.3)	2.17 (± 0.17)	0.59 (± 0.06)	15.8 (± 1.3)	6.4
E136P	1.4 (± 0.1)	17.2 (± 0.8)	12 (± 1)	9.5 (± 0.9)	5.8
A139P	3.1 (± 0.2)	17.3 (± 0.8)	5.6 (± 0.5)	12.2 (± 1.1)	5.8
R143P	4.4 (± 0.3)	54 (± 5)	12.1 (± 1.5)	12.0 (± 1.0)	4.9
D147P	5.0 (± 0.4)	52 (± 4)	10.4 (± 1.1)	12.6 (± 1.1)	4.2
A150P	6.5 (± 0.5)	1090 (± 140)	167 (± 25)	11.0 (± 1.0)	3.6
R154P	7.4 (± 0.5)	2.8 (± 0.2)	0.37 (± 0.04)	11.2 (± 1.0)	2.7
E158P	7.6 (± 0.6)	1.3 (± 0.15)	0.17 (± 0.02)	18.1 (± 1.5)	4.1

Supplementary References

(1) Rogers, J. M.; Steward, A.; Clarke, J. *J Am Chem Soc* **2013**, *135*, 1415.
(2) Day, C. L.; Smits, C.; Fan, F. C.; Lee, E. F.; Fairlie, W. D.; Hinds, M. G. *J Mol Biol* **2008**, *380*, 958.
(3) Munoz, V.; Serrano, L. *J Mol Biol* **1995**, *245*, 297.
(4) Shammas, S. L.; Rogers, J. M.; Hill, S. A.; Clarke, J. *Biophys J* **2012**, *103*, 2203.
(5) Wedemeyer, W. J.; Welker, E.; Scheraga, H. A. *Biochemistry* **2002**, *41*, 14637.